

COMMISSIONING OF THE SEM-GRID MONITORS FOR ELENA

M. McLean*, J. Cenede, G. Tranquille, CERN, Geneva, Switzerland
M. Hori, Max-Planck-Institut für Quantenoptik, Garching, Germany

Abstract

The Extra Low ENergy Antiproton ring (ELENA) is a compact ring for the further deceleration and cooling of the 5.3 MeV antiprotons delivered by the CERN Antiproton Decelerator. It decelerates antiprotons to a minimum energy of 100 keV, creating special challenges for the beam instrumentation. These challenges have been addressed by an extremely sensitive SEM-Grid (Secondary Emission Monitor) monitor which is also compatible with the Ultra High Vacuum (UHV) requirements of ELENA. Since November 2019, ELENA's H^- ion source has been used to test the SEM-Grid monitors and, since July 2020, the monitors have been used to commission the ELENA transfer lines. In this paper, a summary of the features of the SEM-Grid will be given together with an overview of its commissioning activities. An ingenious technique for testing the integrity of the grid wires which are not directly accessible will also be described.

INTRODUCTION

ELENA [1, 2] is a small synchrotron of 30.4 m circumference constructed recently at CERN and sketched in Fig. 1. The purpose of the machine is to decelerate antiprotons coming from the Antiproton Decelerator (AD) [3] at 5.3 MeV beam energy down to 100 keV. Multiple branching electrostatic transfer lines lead to the experimental zones. All the transfer lines are equipped with multiple SEM-Grid Profile Monitors to enable accurate and automated steering of the beam.

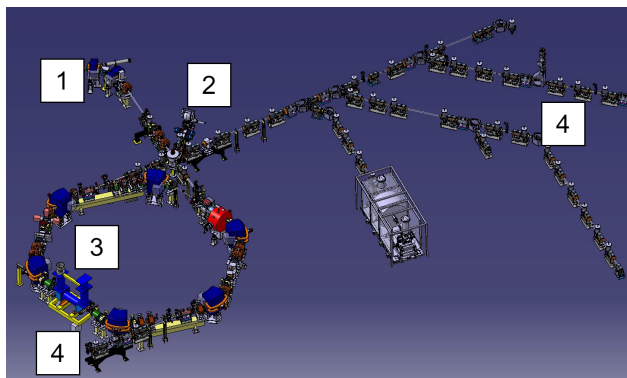


Figure 1: ELENA ring and transfer lines.
1 - Injection from AD
2 - H^- source
3 - ELENA ring with electron cooler
4 - Transfer lines

* mark.mclean@cern.ch

These monitors and electronics were initially developed by the ASACUSA collaboration based on an earlier design [4] used in the radiofrequency quadrupole decelerator facility, and then productionised, assembled, installed, and commissioned by CERN. Numerous issues were resolved during this process. The monitors were installed to observe protons, antiprotons and H^- ions at 100 keV to 5.3 MeV.

MONITOR OVERVIEW AND COMMISSIONING

Each monitor is composed of five stacked grids; one sensor grid for each plane (horizontal and vertical), sandwiched between three anode grids to attract any liberated electrons. The sense grids use 47 wires of $\text{Ø}20\ \mu\text{m}$, while the anode grids use 43 wires of $\text{Ø}12\ \mu\text{m}$. The sense wires are bigger to optimise the charge collection, while the anode wires are a compromise between mechanical strength and beam attenuation. The sense wires are on a $500\ \mu\text{m}$ pitch in the central region and 3 mm pitch at the sides, they are at ground potential. The anode wires are on a 1.5 mm pitch under a bias voltage of 60 V. When a particle hits one of the sensor grid wires, a few electrons are liberated and attracted to the anode wires. A charge then flows into the sensor wire to replace the lost electrons, and this charge is measured. Each monitor absorbs about 10% of the beam, therefore it is mounted on a pneumatic in-out mechanism so it can be removed from the beam path when not required. Figure 2 shows the different components of the SEM-Grid monitor.

A total 43 SEM-Grid Monitors are planned to be installed in the ELENA transfer lines. The installation has been progressing since early 2020, as the transfer lines were completed and as the parts to assemble the monitors became available.

Mechanics

The grids are supported by a guided bellows and connected to the electronics by two 50-way vacuum feedthroughs. All the in-vacuum parts of the monitor were designed to be compliant to stringent vacuum requirements regarding the materials used, the surface treatment and cleanliness, this is especially relevant to the detector grid which utilises a ceramic PCB. The guide rods have a vacuum compatible treatment of molybdenum disulfide (MoS_2) to avoid sticking.

Installation The monitor is assembled in a clean environment and placed in a spare tank to protect the grid during transport. The vertical position of the grid is measured in a metrology laboratory, and any offset is then corrected by a custom spacer. The monitor is then installed in a bake-out

Content from this work must maintain attribution to the author(s), title of the work, publisher, and DOI

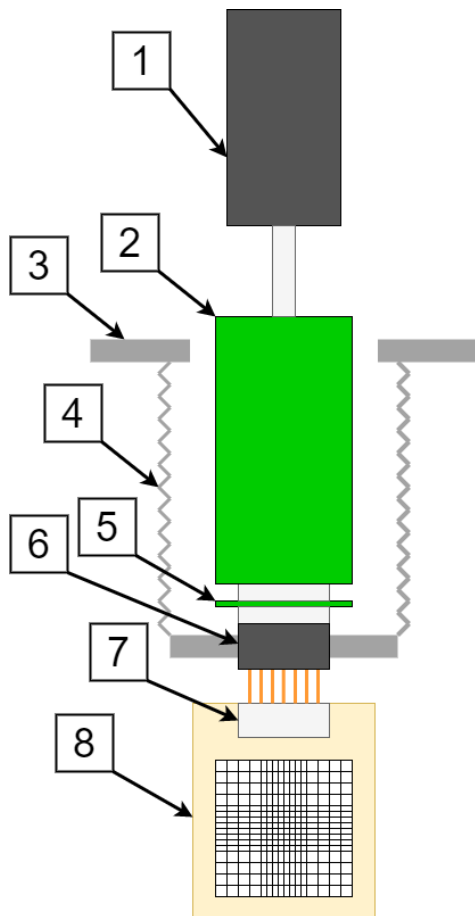


Figure 2: SEM-Grid detector overview. The pneumatic cylinder (1) moves the detector assembly in or out of the beam, while the flange (3) and bellows (4) maintain the vacuum tightness. The front-end boards (2) digitise the extremely weak signals from the detector grid (8), which are connected via an adapter PCB (5), a vacuum feed-through (6) and a D connector (7).

rig and the wires are checked using Time Domain Reflectometry (TDR), described below. If the TDR results are sufficiently good (generally fewer than five non-adjacent bad pairs), the monitor is baked-out at 180 °C for 24 hours under a vacuum. After the bake-out, the temperature is reduced to room temperature and then the pressure should fall to 1×10^{-10} mbar for the monitor to be accepted. The pressure is continuously monitored to detect any leaks and out-gassing must not exceed 2×10^{-8} mbar l/s. Importantly, the temperature is ramped up and down over a period of one day, in order to minimize thermal stress on the delicate sensor grids. Then the TDR test is repeated, and if the results are still acceptable the monitor is ready to be installed.

Key challenges A major challenge with the monitors has been the electrical connections inside the ultra-high-vacuum. The range of available materials is strictly limited, excluding solder flux and conductive epoxy, leaving fluxless soldering or mechanical fastening as the only permitted

techniques. The grid is based on a ceramic Printed Circuit Board (PCB) and the wires are attached by resistance welding. Occasionally a wire may break but this is unusual. The bigger problem, illustrated by Fig. 3, has been the connection of the connector pins to the PCB, this is currently done by vacuum brazing with a fluxless solder with a lead-to-tin ratio of 95%:5% and a melting temperature between $T = 301-314^\circ\text{C}$. We found that the brazing alloy does not adhere very well to the platinum-palladium-gold conductor [6] of the PCB and can fail during the following vacuum bake-out at temperature $T = 180-200^\circ\text{C}$ which typically lasts up to a few days. Oxidization and leaching of the metal alloys at the interface surfaces are assumed to be the primary reasons. No flux can be used during the vacuum brazing to alleviate this problem, as the flux can later contaminate the non-evaporable getter (NEG) pumps of the ELENA beam-lines during bake-out. R&D with other fluxless soldering alloys is ongoing to address this problem.

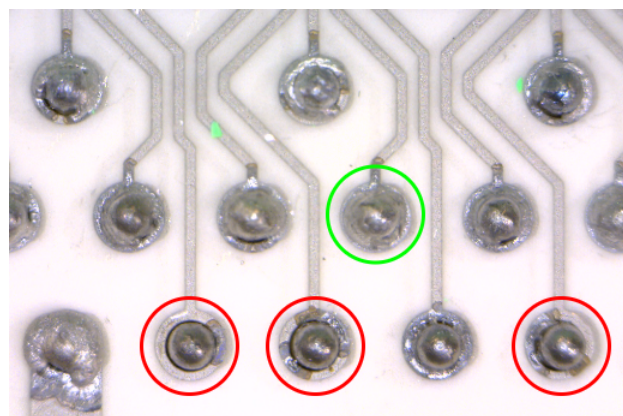


Figure 3: Poor reflow of the fluxless solder indicated by red circles.

Electronics

There is a front-end board for the read-out of each plane. This includes a 64 channel charge sensitive amplifier ASIC (the IDE1140 from IDEAS [5]) which amplifies the signals from all 47 sense wires and simultaneously latches their values in an array of sample-and-holds on receipt of a trigger from the ELENA timing system. These analogue voltages are then converted by a 14 bit ADC under the control of an Field Programmable Gate Array (FPGA). See Figure 4.

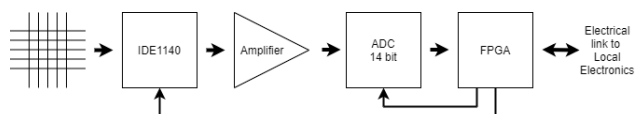


Figure 4: Block diagram of the Front-End.

As shown in Fig. 5, the system is divided in three parts: the front-end boards, a local crate and a VME crate. The front-end boards interface directly to the grids and contain the electronics that amplify and digitise the detector signals. Data and control is exchanged between both front-end boards

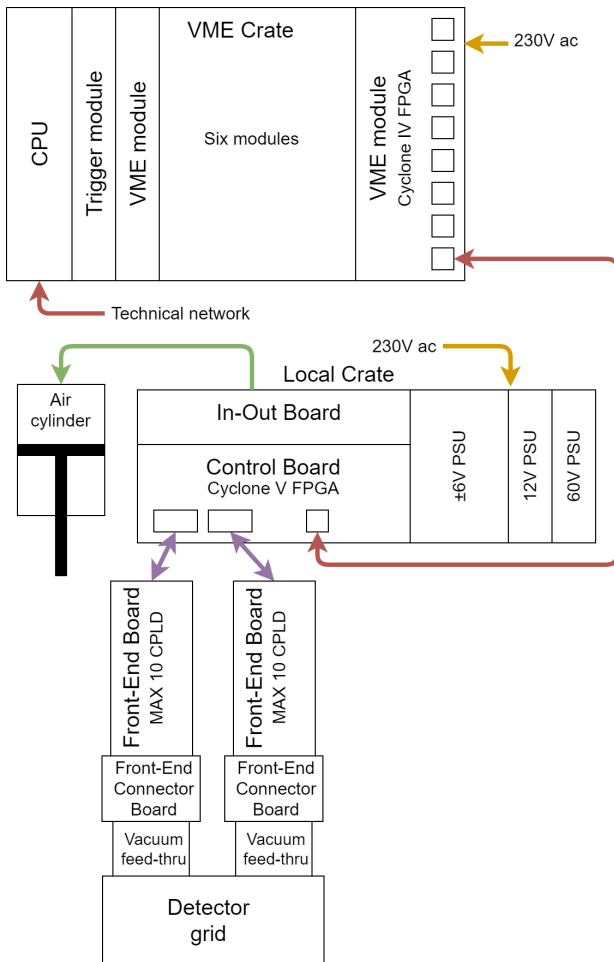


Figure 5: Block diagram of the System.

and the control board in the local crate. In addition, this crate houses the power supplies and the control electronics for the in-out mechanism. From here the data is sent via a fibre-optic cable to a module in a VME crate, where a FESA class (Front-End Software Architecture, the lowest level of CERN's acquisition software stack) provides an interface to the operator's Graphical User Interface (GUI). Each VME module communicates with up to eight monitors. The results are then displayed as horizontal and vertical beam profiles, as shown in Fig. 6, with a Gaussian fit superimposed.

Sensitivity With the H^- source configured to produce small, low-energy bunches, a typical bunch contains about 5×10^6 particles. The sense wires are $\varnothing 20 \mu\text{m}$ on a $500 \mu\text{m}$ pitch, so 4% of the beam hits a sense wire of each plane. A well focused beam has a diameter of 5 mm and so hits about ten wires. Therefore there are about 20,000 beam interactions per wire. A proton of energy $E = 100 \text{ keV}$ striking the Au surface of a sense wire is expected to liberate around 2 secondary electrons [7], which provides a total charge of approximately 6 fC for 20,000 protons. The ASIC (Application Specific Integrated Circuit) noise is about 0.06 fC and the amplifier and ADC (Analogue to Digital Converter) do not add significantly to this. Therefore the expected signal-

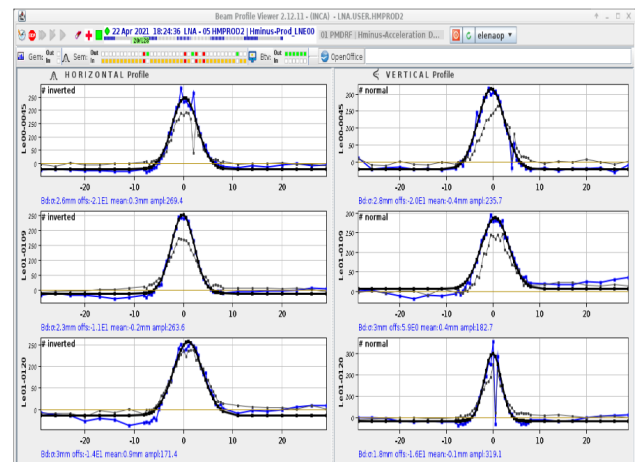


Figure 6: Examples of H^- ion beam profiles.

to-noise ratio is of order 100:1, which correlates well to what has been observed. Tests indicate a similar sensitivity between H^- ions and antiprotons, but the mechanisms by which electrons are liberated in the antiproton case are not fully understood. Besides the contributions from charged pions and nuclear fragments that emerge from antiproton annihilations, there are expected to be some Auger electrons.

There is an offset in the measured signal from each wire, but this offset is stable and the acquisition software records it in the absence of beam and then subtracts it from subsequent readings.

Triggering Timing of the acquisition to better than 500 ns is essential to obtaining a good and repeatable beam profile. Triggers are provided from the H^- source, the injection from the AD, and the two extraction kickers. Once the beam has circulated in ELENA it is split into four bunches. For each monitor, the trigger source and target bunch number can be selected, and there is a programmable delay after which the sample-and-hold circuits of the ASIC are triggered. To tune the delay, a longitudinal acquisition mode is provided in which a single grid wire is sampled continuously at up to 10 MHz. When the results are displayed it is easy to see any adjustment that may be needed to the timing. Figure 7 shows a correctly adjusted delay with the signal peak aligned to time 0. During operation, different bunches may be sent to different transfer lines, so the beam server software updates the bunch number at the start of each cycle.

TIME DOMAIN REFLECTOMETRY (TDR) TESTING OF SENSOR WIRES

One of the recurring challenges during the installation of the SEM-Grids was to verify the condition of the grids when it was not possible to send beam to the monitor. For example, many monitors were installed before the source and ion-switch were fully operational. It was also helpful to be able to verify the grid before the installation of the monitor. In collaboration with our colleagues in the Beam Position Monitoring section we used a handheld Radio-Frequency

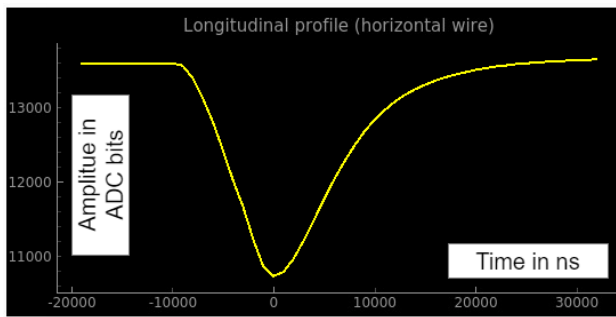


Figure 7: Longitudinal acquisition mode.

(RF) Analyser (the Agilent Fieldfox N9917A) to measure the impedance along an adjacent pair of sensor wires. This was facilitated by a specially designed PCB which routed the sensor wires in pairs from the vacuum feed-through to a matrix of SMA connectors. The impedance of the connection to each pair of sensor wires was then controlled and repeatable. The RF Analyser transmitted a signal at a rapidly swept frequency into the pair of wires, and analysed the echoes returned from each change of impedance. Thus it was possible to compare the impedance of a grid under test with a “known good” grid and easily detect any anomalies in the sensor wire impedance, even for a grid which was installed and under vacuum. This technique could not determine which of the pair of wires was faulty, but it provides a report of how many pairs were faulty. Figure 8 shows an example of data from a grid with a single faulty pair. The early increase of impedance of the orange line is clearly visible.

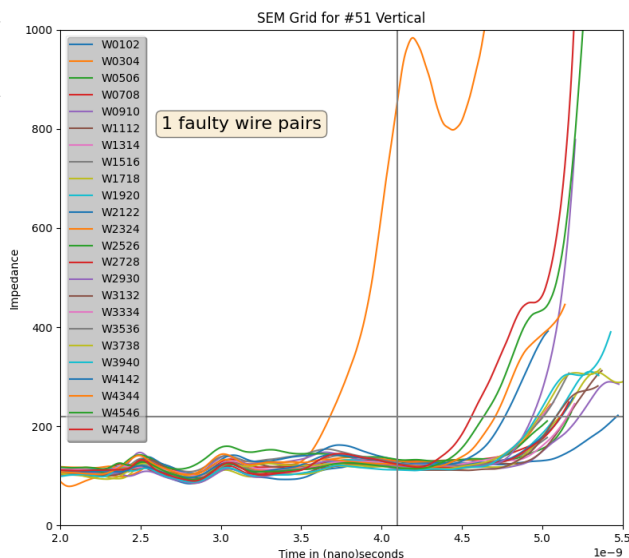


Figure 8: Measurement of impedance against time (=distance) to classify the wire pairs as good or bad.

CONCLUSION

Almost the full complement of SEM-Grid Monitors have now been installed in the ELENA transfer lines and tested with H^- ions. The CERN accelerator complex has restarted this summer and the devices are already providing the ELENA operators with antiproton beam profiles, allowing them to steer the beam to the experiments that will study the symmetry between matter and antimatter.

ACKNOWLEDGEMENTS

None of this would have been possible without the help and support of: Arkadiusz Jedrzej Lis and Stephane Bart Pedersen of the SY-BI-SW software section; Alexander Sinturel of TE-VSC vacuum group; Laurette Ponce, Davide Gamba and the rest of the BE-OP-AD operations team; Stephane Deschamps, Wilfried Devauchelle and the rest of the SY-BI-XEI section; Christian Carli and Francois Butin who kept us focused.

REFERENCES

- [1] V. Chohan *et al.*, “Extra Low ENergy Antiproton (ELENA) ring and its Transfer Lines”, CERN, Geneva, Switzerland, Rep. CERN-2014-002, April 2014.
- [2] C. Carli *et al.*, “ELENA Commissioning and Status”, presented at the 12th Int. Particle Accelerator Conf. (IPAC’21), Campinas, Brazil, May 2021, paper MOPAB177.
- [3] Antiproton decelerator, <https://home.cern/science/accelerators/antiproton-decelerator/>.
- [4] M. Hori, “Photocathode microwire monitor for nondestructive and highly sensitive spatial profile measurements of ultraviolet, x-ray, and charged particle beams”, *Rev. Sci. Instrum.*, vol. 75, p. 113303, 2005.
- [5] Integrated Detector Electronics AS, <http://ideas.no/products/ide1140/>.
- [6] Dupont 4597R, <https://www.dupont.com/content/dam/dupont/amer/us/en/transportation-industrial/public/documents/en/4597R.pdf>
- [7] D. Hasselkamp, K.G. Lang, A. Scharmann, N. Stiller, “Ion induced electron emission from metal surfaces”, *Nucl. Instrum. Methods*, vol. 180, p. 349, 1981.